

## Updated cross section measurement of $e^+e^- \rightarrow K^+K^-J/\psi$ and $K_S^0K_S^0J/\psi$ via initial state radiation at Belle

C. P. Shen,<sup>2</sup> C. Z. Yuan,<sup>18</sup> P. Wang,<sup>18</sup> A. Abdesselam,<sup>57</sup> I. Adachi,<sup>13</sup> H. Aihara,<sup>62</sup> S. Al Said,<sup>57,27</sup> D. M. Asner,<sup>49</sup> V. Aulchenko,<sup>4</sup> T. Aushev,<sup>22</sup> R. Ayad,<sup>57</sup> A. M. Bakich,<sup>56</sup> A. Bala,<sup>50</sup> A. Bobrov,<sup>4</sup> G. Bonvicini,<sup>68</sup> A. Bozek,<sup>44</sup> M. Bračko,<sup>34,23</sup> T. E. Browder,<sup>12</sup> V. Chekelian,<sup>35</sup> A. Chen,<sup>41</sup> B. G. Cheon,<sup>11</sup> K. Chilikin,<sup>22</sup> R. Chistov,<sup>22</sup> K. Cho,<sup>28</sup> V. Chobanova,<sup>35</sup> S.-K. Choi,<sup>10</sup> Y. Choi,<sup>55</sup> D. Cinabro,<sup>68</sup> J. Dalseno,<sup>35,59</sup> M. Danilov,<sup>22,37</sup> Z. Doležal,<sup>5</sup> A. Drutskoy,<sup>22,37</sup> D. Dutta,<sup>16</sup> S. Eidelman,<sup>4</sup> D. Epifanov,<sup>62</sup> H. Farhat,<sup>68</sup> J. E. Fast,<sup>49</sup> T. Ferber,<sup>7</sup> A. Frey,<sup>9</sup> V. Gaur,<sup>58</sup> S. Ganguly,<sup>68</sup> R. Gillard,<sup>68</sup> R. Glattauer,<sup>19</sup> Y. M. Goh,<sup>11</sup> B. Golob,<sup>32,23</sup> J. Haba,<sup>13</sup> K. Hayasaka,<sup>39</sup> H. Hayashii,<sup>40</sup> X. H. He,<sup>51</sup> Y. Hoshi,<sup>60</sup> W.-S. Hou,<sup>43</sup> Y. B. Hsiung,<sup>43</sup> H. J. Hyun,<sup>30</sup> T. Iijima,<sup>39,38</sup> A. Ishikawa,<sup>61</sup> R. Itoh,<sup>13</sup> Y. Iwasaki,<sup>13</sup> D. Joffe,<sup>25</sup> T. Julius,<sup>36</sup> J. H. Kang,<sup>70</sup> E. Kato,<sup>61</sup> T. Kawasaki,<sup>46</sup> C. Kiesling,<sup>35</sup> D. Y. Kim,<sup>54</sup> H. J. Kim,<sup>30</sup> J. B. Kim,<sup>29</sup> J. H. Kim,<sup>28</sup> K. T. Kim,<sup>29</sup> M. J. Kim,<sup>30</sup> Y. J. Kim,<sup>28</sup> K. Kinoshita,<sup>6</sup> B. R. Ko,<sup>29</sup> P. Kodyš,<sup>5</sup> S. Korpar,<sup>34,23</sup> P. Križan,<sup>32,23</sup> P. Krokovny,<sup>4</sup> A. Kuzmin,<sup>4</sup> Y.-J. Kwon,<sup>70</sup> S.-H. Lee,<sup>29</sup> J. Li,<sup>53</sup> L. Li Gioi,<sup>35</sup> J. Libby,<sup>17</sup> C. Liu,<sup>52</sup> Z. Q. Liu,<sup>18</sup> P. Lukin,<sup>4</sup> D. Matvienko,<sup>4</sup> K. Miyabayashi,<sup>40</sup> H. Miyata,<sup>46</sup> R. Mizuk,<sup>22,37</sup> A. Moll,<sup>35,59</sup> R. Mussa,<sup>21</sup> Y. Nagasaka,<sup>14</sup> E. Nakano,<sup>48</sup> M. Nakao,<sup>13</sup> Z. Natkaniec,<sup>44</sup> M. Nayak,<sup>17</sup> E. Nedelkovska,<sup>35</sup> N. K. Nisar,<sup>58</sup> S. Nishida,<sup>13</sup> O. Nitoh,<sup>65</sup> S. Okuno,<sup>24</sup> C. W. Park,<sup>55</sup> H. Park,<sup>30</sup> T. K. Pedlar,<sup>33</sup> R. Pestotnik,<sup>23</sup> M. Petrič,<sup>23</sup> L. E. Piilonen,<sup>67</sup> M. Ritter,<sup>35</sup> M. Röhrken,<sup>26</sup> A. Rostomyan,<sup>7</sup> S. Ryu,<sup>53</sup> T. Saito,<sup>61</sup> Y. Sakai,<sup>13</sup> T. Sanuki,<sup>61</sup> Y. Sato,<sup>61</sup> O. Schneider,<sup>31</sup> G. Schnell,<sup>1,15</sup> D. Semmler,<sup>8</sup> K. Senyo,<sup>69</sup> O. Seon,<sup>38</sup> M. E. Sevier,<sup>36</sup> M. Shapkin,<sup>20</sup> V. Shebalin,<sup>4</sup> T.-A. Shibata,<sup>63</sup> J.-G. Shiu,<sup>43</sup> B. Shwartz,<sup>4</sup> A. Sibidanov,<sup>56</sup> F. Simon,<sup>35,59</sup> Y.-S. Sohn,<sup>70</sup> A. Sokolov,<sup>20</sup> E. Solovieva,<sup>22</sup> S. Stanič,<sup>47</sup> M. Starič,<sup>23</sup> M. Steder,<sup>7</sup> T. Sumiyoshi,<sup>64</sup> U. Tamponi,<sup>21,66</sup> G. Tatishvili,<sup>49</sup> Y. Teramoto,<sup>48</sup> M. Uchida,<sup>63</sup> Y. Unno,<sup>11</sup> S. Uno,<sup>13</sup> P. Urquijo,<sup>3</sup> Y. Usov,<sup>4</sup> C. Van Hulse,<sup>1</sup> P. Vanhoefer,<sup>35</sup> G. Varner,<sup>12</sup> V. Vorobyev,<sup>4</sup> M. N. Wagner,<sup>8</sup> C. H. Wang,<sup>42</sup> M. Watanabe,<sup>46</sup> Y. Watanabe,<sup>24</sup> K. M. Williams,<sup>67</sup> E. Won,<sup>29</sup> H. Yamamoto,<sup>61</sup> Y. Yamashita,<sup>45</sup> S. Yashchenko,<sup>7</sup> Y. Yook,<sup>70</sup> C. C. Zhang,<sup>18</sup> Z. P. Zhang,<sup>52</sup> V. Zhulanov,<sup>4</sup> and A. Zupanc<sup>23</sup>

(Belle Collaboration)

<sup>1</sup>University of the Basque Country UPV/EHU, 48080 Bilbao

<sup>2</sup>Beihang University, Beijing 100191

<sup>3</sup>University of Bonn, 53115 Bonn

<sup>4</sup>Budker Institute of Nuclear Physics SB RAS and Novosibirsk State University, Novosibirsk 630090

<sup>5</sup>Faculty of Mathematics and Physics, Charles University, 121 16 Prague

<sup>6</sup>University of Cincinnati, Cincinnati, Ohio 45221

<sup>7</sup>Deutsches Elektronen-Synchrotron, 22607 Hamburg

<sup>8</sup>Justus-Liebig-Universität Gießen, 35392 Gießen

<sup>9</sup>II. Physikalisches Institut, Georg-August-Universität Göttingen, 37073 Göttingen

<sup>10</sup>Gyeongsang National University, Chinju 660-701

<sup>11</sup>Hanyang University, Seoul 133-791

<sup>12</sup>University of Hawaii, Honolulu, Hawaii 96822

<sup>13</sup>High Energy Accelerator Research Organization (KEK), Tsukuba 305-0801

<sup>14</sup>Hiroshima Institute of Technology, Hiroshima 731-5193

<sup>15</sup>IKERBASQUE, Basque Foundation for Science, 48011 Bilbao

<sup>16</sup>Indian Institute of Technology Guwahati, Assam 781039

<sup>17</sup>Indian Institute of Technology Madras, Chennai 600036

<sup>18</sup>Institute of High Energy Physics, Chinese Academy of Sciences, Beijing 100049

<sup>19</sup>Institute of High Energy Physics, Vienna 1050

<sup>20</sup>Institute for High Energy Physics, Protvino 142281

<sup>21</sup>INFN - Sezione di Torino, 10125 Torino

<sup>22</sup>Institute for Theoretical and Experimental Physics, Moscow 117218

<sup>23</sup>J. Stefan Institute, 1000 Ljubljana

<sup>24</sup>Kanagawa University, Yokohama 221-8686

<sup>25</sup>Kennesaw State University, Kennesaw, Georgia 30144

<sup>26</sup>Institut für Experimentelle Kernphysik, Karlsruher Institut für Technologie, 76131 Karlsruhe

<sup>27</sup>Department of Physics, Faculty of Science, King Abdulaziz University, Jeddah 21589

<sup>28</sup>Korea Institute of Science and Technology Information, Daejeon 305-806

<sup>29</sup>Korea University, Seoul 136-713

<sup>30</sup>Kyungpook National University, Daegu 702-701

<sup>31</sup>École Polytechnique Fédérale de Lausanne (EPFL), Lausanne 1015

<sup>32</sup>Faculty of Mathematics and Physics, University of Ljubljana, 1000 Ljubljana

- <sup>33</sup>Luther College, Decorah, Iowa 52101  
<sup>34</sup>University of Maribor, 2000 Maribor  
<sup>35</sup>Max-Planck-Institut für Physik, 80805 München  
<sup>36</sup>School of Physics, University of Melbourne, Victoria 3010  
<sup>37</sup>Moscow Physical Engineering Institute, Moscow 115409  
<sup>38</sup>Graduate School of Science, Nagoya University, Nagoya 464-8602  
<sup>39</sup>Kobayashi-Maskawa Institute, Nagoya University, Nagoya 464-8602  
<sup>40</sup>Nara Women's University, Nara 630-8506  
<sup>41</sup>National Central University, Chung-li 32054  
<sup>42</sup>National United University, Miao Li 36003  
<sup>43</sup>Department of Physics, National Taiwan University, Taipei 10617  
<sup>44</sup>H. Niewodniczanski Institute of Nuclear Physics, Krakow 31-342  
<sup>45</sup>Nippon Dental University, Niigata 951-8580  
<sup>46</sup>Niigata University, Niigata 950-2181  
<sup>47</sup>University of Nova Gorica, 5000 Nova Gorica  
<sup>48</sup>Osaka City University, Osaka 558-8585  
<sup>49</sup>Pacific Northwest National Laboratory, Richland, Washington 99352  
<sup>50</sup>Panjab University, Chandigarh 160014  
<sup>51</sup>Peking University, Beijing 100871  
<sup>52</sup>University of Science and Technology of China, Hefei 230026  
<sup>53</sup>Seoul National University, Seoul 151-742  
<sup>54</sup>Soongsil University, Seoul 156-743  
<sup>55</sup>Sungkyunkwan University, Suwon 440-746  
<sup>56</sup>School of Physics, University of Sydney, New South Wales 2006  
<sup>57</sup>Department of Physics, Faculty of Science, University of Tabuk, Tabuk 71451  
<sup>58</sup>Tata Institute of Fundamental Research, Mumbai 400005  
<sup>59</sup>Excellence Cluster Universe, Technische Universität München, 85748 Garching  
<sup>60</sup>Tohoku Gakuin University, Tagajo 985-8537  
<sup>61</sup>Tohoku University, Sendai 980-8578  
<sup>62</sup>Department of Physics, University of Tokyo, Tokyo 113-0033  
<sup>63</sup>Tokyo Institute of Technology, Tokyo 152-8550  
<sup>64</sup>Tokyo Metropolitan University, Tokyo 192-0397  
<sup>65</sup>Tokyo University of Agriculture and Technology, Tokyo 184-8588  
<sup>66</sup>University of Torino, 10124 Torino  
<sup>67</sup>CNP, Virginia Polytechnic Institute and State University, Blacksburg, Virginia 24061  
<sup>68</sup>Wayne State University, Detroit, Michigan 48202  
<sup>69</sup>Yamagata University, Yamagata 990-8560  
<sup>70</sup>Yonsei University, Seoul 120-749

(Received 26 February 2014; published 23 April 2014)

The cross sections of the processes  $e^+e^- \rightarrow K^+K^-J/\psi$  and  $K_S^0\bar{K}_S^0J/\psi$  are measured via initial state radiation at center-of-mass energies between the threshold and 6.0 GeV using a data sample of 980 fb<sup>-1</sup> collected with the Belle detector on or near the  $\Upsilon(nS)$  resonances, where  $n = 1, 2, \dots, 5$ . The cross sections for  $e^+e^- \rightarrow K^+K^-J/\psi$  are at a few pb level and the average cross section for  $e^+e^- \rightarrow K_S^0\bar{K}_S^0J/\psi$  is  $1.8 \pm 0.6(\text{stat}) \pm 0.3(\text{syst})$  pb between 4.4 and 5.2 GeV. All of them are consistent with previously published results with improved precision. A search for resonant structures and associated intermediate states in the cross section of the process  $e^+e^- \rightarrow K^+K^-J/\psi$  is performed.

DOI: 10.1103/PhysRevD.89.072015

PACS numbers: 14.40.Rt, 13.25.Gv, 13.66.Bc

## I. INTRODUCTION

Recently a new charged charmoniumlike state, the  $Z(3900)^\pm$ , was observed by the Belle [1] and BESIII [2] experiments in a study of  $e^+e^- \rightarrow \pi^+\pi^-J/\psi$  at center-of-mass (CM) energies around 4.26 GeV. It was soon confirmed with the CLEO data at a CM energy of 4.17 GeV [3]. As the  $Z(3900)^\pm$  state has a strong coupling to charmonium and is charged, it cannot be a conventional

charmonium state. This observation has stimulated a number of distinct interpretations. These include a tetraquark state [4],  $D\bar{D}^*$  molecule [5], hadroquarkonium [6], and other configurations [7]. More recently, BESIII observed another charged charmoniumlike state,  $Z_c(4020)^\pm$ , in  $e^+e^- \rightarrow \pi^+\pi^-h_c$  [8]. These states, together with similar states observed in the bottomonium system [9], indicate the existence of a new class of hadrons.

A strange partner of the  $Z(3900)^\pm$ , called  $Z_{cs}$ , may exist in the above scenarios. The mass of a  $J^P = 1^+ D_s \bar{D}^*$  molecular state was first predicted [10] using QCD sum rules with  $M(Z_{cs}) = (3.97 \pm 0.08) \text{ GeV}/c^2$ , which is very close to the  $D_s^+ \bar{D}^{*0}$  threshold of  $3.976 \text{ GeV}/c^2$ . Using the same QCD sum rules, the authors of Ref. [11] calculated the decay widths of the  $Z_{cs}^+$  to  $K^+ J/\psi$ ,  $K^{*+} \eta_c$ ,  $D_s^+ \bar{D}^{*0}$  and  $\bar{D}^0 D_s^{*+}$ , assuming the  $Z_{cs}$  to be a tetraquark state. Such a state is also predicted in the single-kaon emission model [12].

Using a data sample of  $673 \text{ fb}^{-1}$  collected at or near  $\sqrt{s} = 10.58 \text{ GeV}$ , Belle has observed abundant  $e^+e^- \rightarrow K^+K^-J/\psi$  signal events via initial state radiation (ISR) [13]. In addition, there is one very broad structure in the  $K^+K^-J/\psi$  mass spectrum; fits using either a single Breit-Wigner (BW) function, or the  $\psi(4415)$  plus a second BW function yield resonant parameters that are very different from those of the currently tabulated excited  $\psi$  states [14]. Unfortunately, the  $M(K^\pm J/\psi)$  distribution is not shown in Ref. [13].

In this paper, we report the updated measurement of the cross sections for  $e^+e^- \rightarrow K^+K^-J/\psi$  and  $K_S^0 K_S^0 J/\psi$  between threshold and  $6.0 \text{ GeV}$  and examine possible resonant structures in the cross section of the process  $e^+e^- \rightarrow K^+K^-J/\psi$  as well as in the  $K^\pm J/\psi$  and  $K^+K^-$  systems. The results are based on the full Belle data sample with an integrated luminosity of  $980 \text{ fb}^{-1}$  collected on or near the  $\Upsilon(nS)$  ( $n = 1, 2, \dots, 5$ ).

The Belle detector at the KEKB asymmetric-energy  $e^+e^-$  collider [15] is described in detail elsewhere [16]. This analysis supersedes that reported in Ref. [13] where a subset of the Belle data sample was used.

We use the PHOKHARA [17] program to generate signal Monte Carlo (MC) events and determine experimental efficiencies. In the generator, one or two photons are allowed to be emitted before forming the resonance  $X$ ; then  $X$  decays into  $K^+K^-J/\psi$  with  $J/\psi$  decaying into  $\ell^+\ell^-$  ( $\ell = e$  or  $\mu$ ). When generating the MC sample, the mass of  $X$  is fixed to a certain value while the width is set to zero. In  $X \rightarrow K^+K^-J/\psi$ , a pure  $S$  wave between the  $K^+K^-$  system and the  $J/\psi$  as well as between the  $K^+$  and  $K^-$  is assumed. The invariant mass of the  $K^+K^-$  system is generated uniformly in phase space. To estimate the model uncertainty, we also generate events with a  $K^+K^-$  invariant mass distributed like  $M(\pi^+\pi^-)$  in  $\psi(2S) \rightarrow \pi^+\pi^-J/\psi$  decays [18].

## II. EVENT SELECTION

The selection of  $K^+K^-\ell^+\ell^-$  events is the same as in Ref. [13]. For the events of interest, we require four well-reconstructed charged tracks with zero net charge. The impact parameters of these tracks perpendicular to and along the beam direction with respect to the interaction point are required to be less than  $0.5$  and  $4.0 \text{ cm}$ , respectively. For each charged track, a combined likelihood

ratio from various detector subsystems is formed to identify different particle species ( $e, \mu, \pi, K, p$ ). Tracks with  $\mathcal{R}_K = \frac{\mathcal{L}_K}{\mathcal{L}_K + \mathcal{L}_\pi} > 0.6$  are identified as kaons with an efficiency of about 92%; about 4% are misidentified pions [19]. Similar ratios are also defined for leptons [20,21]. For electrons from  $J/\psi \rightarrow e^+e^-$ , one track should have  $\mathcal{R}_e > 0.95$  and the other  $\mathcal{R}_e > 0.05$ ; for muons from  $J/\psi \rightarrow \mu^+\mu^-$ , at least one track should have  $\mathcal{R}_\mu > 0.95$ ; in cases where the other has no muon identification ( $\mathcal{R}_\mu = 0$ ), in order to suppress fake muon tracks, the cosine of the polar angle of each muon track in the  $K^+K^-\mu^+\mu^-$  CM frame is required to be less than  $0.7$ . Events with  $\gamma$  conversions are removed by requiring  $\mathcal{R}_e < 0.75$  for the  $K^+K^-$  tracks. In  $J/\psi \rightarrow e^+e^-$ ,  $\gamma$  conversion events are further suppressed by requiring the invariant mass of  $K^+K^-$  to be larger than  $1.05 \text{ GeV}/c^2$ ; this also removes the events with a  $\phi$  meson in the final state. In  $J/\psi \rightarrow \mu^+\mu^-$ , the invariant mass of  $K^+K^-$  is required to be outside a  $\pm 10 \text{ MeV}/c^2$  interval around the  $\phi$  nominal mass to remove events with a  $\phi$  meson in the final state, possibly produced via  $e^+e^- \rightarrow \gamma\gamma^*\gamma^* \rightarrow \gamma\phi\ell^+\ell^-$ . There is only one combination of  $K^+K^-\ell^+\ell^-$  in each event after the above event selections.

The ISR events are identified by the requirement  $|M_{\text{rec}}^2| < 1.0 (\text{GeV}/c^2)^2$ , where  $M_{\text{rec}}^2 = (P_{\text{CM}} - P_{K^+} - P_{K^-} - P_{\ell^+} - P_{\ell^-})^2$  and  $P_i$  represents the four-momentum of the corresponding particle in the  $e^+e^-$  CM frame. Clear  $J/\psi$  signals are observed in both  $J/\psi \rightarrow e^+e^-$  and  $J/\psi \rightarrow \mu^+\mu^-$  modes, as shown in Fig. 1. We define the  $J/\psi$  signal region as  $3.06 < M(\ell^+\ell^-) < 3.14 \text{ GeV}/c^2$  (with the mass resolution of lepton pairs being about  $17 \text{ MeV}/c^2$ ), and the  $J/\psi$  mass sideband as  $2.91 < M(\ell^+\ell^-) < 3.03$  or  $3.17 < M(\ell^+\ell^-) < 3.29 \text{ GeV}/c^2$ , which is three times the width of the signal region. Here, final state radiation and bremsstrahlung energy loss are recovered by adding the four-momentum of photons detected within a  $5^\circ$  cone around the electron and positron direction in the  $e^+e^-$  invariant mass calculation.

For selection of  $e^+e^- \rightarrow K_S^0 K_S^0 \ell^+\ell^-$  events within the same data sample, all the selection criteria are the same as for  $K^+K^-J/\psi$  except that the selection of  $K^+K^-$  is replaced by the selection of two  $K_S^0$ . For a  $K_S^0$  candidate decaying into  $\pi^+\pi^-$ , we require that the invariant mass of the  $\pi^+\pi^-$  pair lie within a  $\pm 11 \text{ MeV}/c^2$  interval around the  $K_S^0$  nominal mass, which contains around 95% of the signal according to the MC simulation, and that the pion pair has a displaced vertex and flight direction consistent with a  $K_S^0$  originating from the interaction point [22].

Figure 2 shows the  $K^+K^-\ell^+\ell^-$  and  $K_S^0 K_S^0 \ell^+\ell^-$  invariant mass [23] distributions after applying the above selection, together with the backgrounds estimated from the normalized  $J/\psi$  mass sidebands. The  $K^+K^-\ell^+\ell^-$  invariant mass distribution is similar to that in Ref. [13] and shows a broad enhancement around  $4.4\text{--}5.5 \text{ GeV}/c^2$ . In addition, there are three events near  $\sqrt{s} = 4.26 \text{ GeV}$ . It

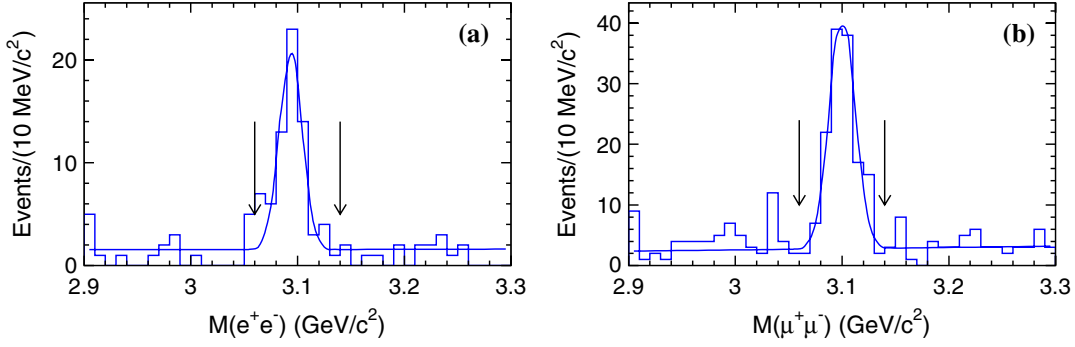


FIG. 1 (color online). Invariant mass distributions of (a)  $e^+e^-$  and (b)  $\mu^+\mu^-$  for selected  $K^+K^-\ell^+\ell^-$  candidates. The curves show the best fits to the mass spectra, and the arrows show the required  $J/\psi$  signal regions defined in the text.

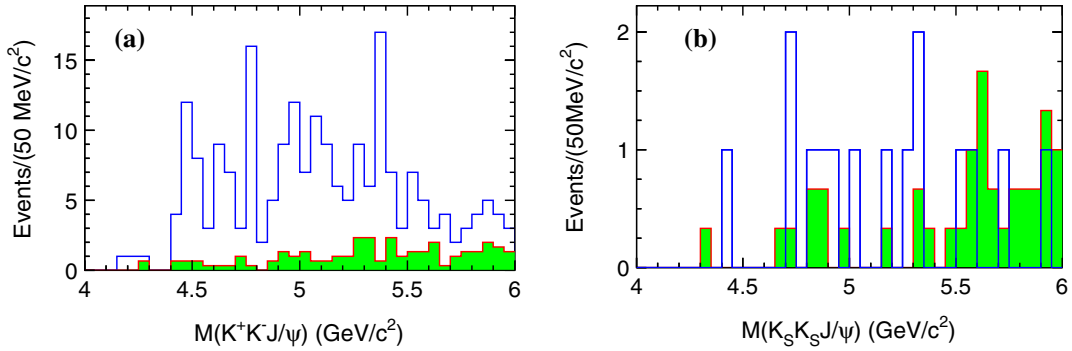


FIG. 2 (color online). The invariant mass distributions of the  $K^+K^-J/\psi$  (a) and  $K_S^0K_S^0J/\psi$  (b) candidates. The open histograms are from the  $J/\psi$  signal region, while the shaded ones are from the  $J/\psi$  mass sideband regions after a proper normalization.

is evident from the figure that the background estimated from the  $J/\psi$  mass sidebands is low, which indicates that the background from the non- $J/\psi$  final states is small. The other backgrounds not shown in the sidebands include (1)  $K^+K^-J/\psi$  with  $J/\psi$  decaying into final states other than lepton pairs; (2)  $XJ/\psi$ , with  $X$  not being  $K^+K^-$ , such

as  $\pi^+\pi^-$ . The number of these background events is found to be small from MC simulation and thus they are neglected. Non-ISR production of the  $e^+e^- \rightarrow K^+K^-J/\psi$  process, such as  $e^+e^- \rightarrow \gamma\gamma^*\gamma^* \rightarrow \gamma\phi J/\psi$ , is calculated to be small [24] and is neglected. For the  $M(K_S^0K_S^0J/\psi)$  distribution, there are only ten signal

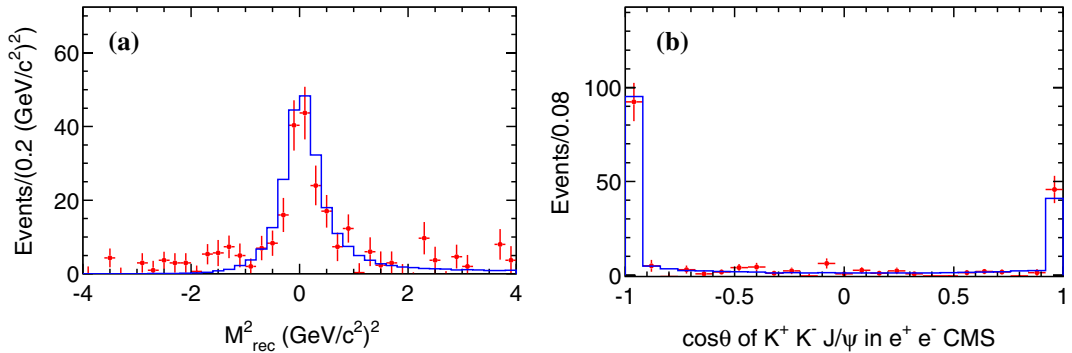


FIG. 3 (color online). (a) The distribution of the squared mass recoiling against the  $K^+K^-J/\psi$  system distribution and (b) the polar angle distribution of the  $K^+K^-J/\psi$  system in the  $e^+e^-$  CM frame for the selected  $K^+K^-J/\psi$  events with invariant masses between 4.0 and 6.0  $\text{GeV}/c^2$ . The points with error bars are data with the normalized  $J/\psi$  mass sidebands subtracted; the solid histograms are MC simulated events.

candidate events between 4.6 and 5.5 GeV/ $c^2$  with four background events estimated from the  $J/\psi$  mass sidebands. In other regions, the number of events in the  $J/\psi$  signal region is about the same as expected from the normalized sideband events.

Figures 3(a) and (b) show the distribution of the squared mass recoiling against the  $K^+K^-J/\psi$  system and the polar angle distribution of the  $K^+K^-J/\psi$  system in the  $e^+e^-$  CM frame, respectively, for the selected  $K^+K^-J/\psi$  events with invariant masses between 4.0 and 6.0 GeV/ $c^2$ . The data, shown with the normalized  $J/\psi$  mass sidebands subtracted, agree well with the MC simulation (open histograms), indicating the existence of signals that are produced from ISR.

### III. CROSS SECTIONS

The  $e^+e^- \rightarrow K^+K^-J/\psi$  cross section at each energy point is calculated using

$$\sigma_i = \frac{n_i^{\text{obs}} - f \times n_i^{\text{bkg}}}{\mathcal{L}_i \cdot \epsilon_i \cdot \mathcal{B}(J/\psi \rightarrow \ell^+\ell^-)},$$

where  $n_i^{\text{obs}}$ ,  $n_i^{\text{bkg}}$ ,  $f$ ,  $\epsilon_i$ , and  $\mathcal{L}_i$  are the number of observed events in data, the number of background events estimated from the  $J/\psi$  sidebands, the scale factor ( $f = 1/3$ ), the detection efficiency, and the effective ISR luminosity obtained from the QED calculation [25] in the  $i$ th energy bin, respectively;  $\mathcal{B}(J/\psi \rightarrow \ell^+\ell^-) = 11.87\%$  is taken from Ref. [14]. According to the MC simulation, the efficiency for  $K^+K^-J/\psi$  ( $K_S^0K_S^0J/\psi$ ) increases smoothly from 1.69% (0.30%) at 4.2 GeV/ $c^2$ , 7.53% (0.56%) at 4.6 GeV/ $c^2$ , 11.50% (1.04%) at 5.2 GeV/ $c^2$ , to 14.93% (1.45%) at 5.8 GeV/ $c^2$ . Figure 4 shows the measured cross sections for  $e^+e^- \rightarrow K^+K^-J/\psi$ , where the error bars indicate the combined statistical errors of the signal and the background events, following the procedure in

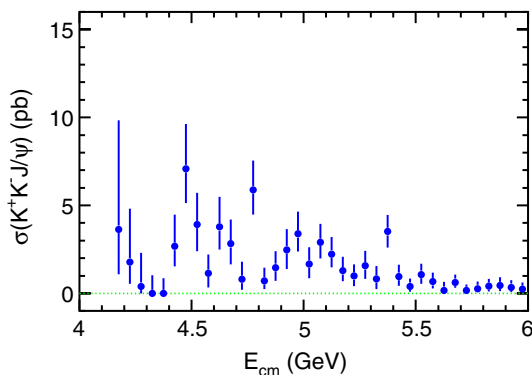


FIG. 4 (color online). The measured  $e^+e^- \rightarrow K^+K^-J/\psi$  cross sections for CM energies up to 6.0 GeV (points with error bars). The errors are statistical and are determined by the numbers of signal and background events; a 7.8% systematic error that is common for all data points is not included.

Ref. [26]. The measured  $e^+e^- \rightarrow K^+K^-J/\psi$  cross sections are consistent with previously published results [13] with improved precision. Similarly, the  $e^+e^- \rightarrow K_S^0K_S^0J/\psi$  cross section is calculated. Since the number of  $K_S^0K_S^0J/\psi$  signal events is very small, we give an average cross section for  $e^+e^- \rightarrow K_S^0K_S^0J/\psi$  of  $1.8 \pm 0.6(\text{stat})$  pb between 4.4 and 5.2 GeV/ $c^2$ . The result is consistent with the previously published result of  $1.8^{+1.4}_{-1.1}(\text{stat})$  pb [13] with better precision. Tables I and II list the final results and all the information used in the cross section calculation for  $e^+e^- \rightarrow K^+K^-J/\psi$  and  $K_S^0K_S^0J/\psi$ , respectively.

Systematic error sources and their contributions in the cross section measurements are summarized in Table III. The lepton pair identification uncertainties, measured from a pure control sample of  $e^+e^- \rightarrow \gamma_{\text{ISR}}\psi(2S)$  events with  $\psi(2S) \rightarrow \pi^+\pi^-J/\psi$ ,  $J/\psi \rightarrow \ell^+\ell^-$ , are 3.5% and 1.8% for  $e^+e^-$  and  $\mu^+\mu^-$ , respectively [1]. The uncertainty due to kaon particle identification is 1.2% for each kaon. Tracking efficiency uncertainties are estimated to be 1.3% per kaon track and 0.35% per lepton track, which are fully correlated in the momentum and angle regions of interest for signal events. The systematic uncertainty in the  $K_S^0$  reconstruction efficiency is estimated by using the control samples of reconstructed  $D^{*\pm}$  decays with the decay chain  $D^{*\pm} \rightarrow \pi_s^\pm D^0$ ,  $D^0 \rightarrow K_S^0\pi^+\pi^-$ . We find that the MC efficiency is higher than in data by  $(2.1 \pm 0.7)\%$ . We take 2.8% as the systematic uncertainty for each  $K_S^0$  selection. The uncertainties associated with the  $J/\psi$  mass window and  $|M_{\text{rec}}^2|$  requirements are also estimated using pure  $\psi(2S) \rightarrow \pi^+\pi^-J/\psi$  events. It is found that MC efficiencies are higher than in data by  $(4.5 \pm 0.4)\%$  in the  $e^+e^-$  mode and  $(4.1 \pm 0.2)\%$  in the  $\mu^+\mu^-$  mode. The differences in efficiencies are corrected and the uncertainties in the correction factors are taken as systematic errors. They contribute 0.6% for the  $e^+e^-$  and 0.3% for the  $\mu^+\mu^-$  mode in total for the  $J/\psi$  mass window together with the  $|M_{\text{rec}}^2|$  requirements [1]. Estimating the backgrounds using different  $J/\psi$  mass sidebands results in a change of background events at the 0.12/50 MeV/ $c^2$  level for  $K^+K^-J/\psi$  and at the 0.008/50 MeV/ $c^2$  level for  $K_S^0K_S^0J/\psi$ , corresponding to an average change of about 2.6% for  $K^+K^-J/\psi$  and 14% for  $K_S^0K_S^0J/\psi$  in the cross section. Belle measures the total luminosity with a precision of 1.4% using Bhabha events. The PHOKHARA generator calculates the ISR photon radiator function with 0.1% accuracy [17]. The dominant uncertainties due to the generator come from the three-body decay dynamics; there is no good model to describe the  $K^+K^-$  invariant mass spectrum. Simulations with modified  $K^+K^-$  invariant mass distributions such as  $M(\pi^+\pi^-)$  in  $\psi(2S) \rightarrow \pi^+\pi^-J/\psi$  [18] yield efficiencies that are higher by 3.3%–4.8% for different  $K^+K^-J/\psi$  masses. We take 4.8% as a conservative estimation for the  $K^+K^-J/\psi$  mass values. Similarly, we take 4.5% for the  $K_S^0K_S^0J/\psi$  mode. The angular distributions of the final state particles for selected  $K^+K^-J/\psi$  events from data are consistent with the

TABLE I. Cross sections ( $\sigma$ ) of  $e^+e^- \rightarrow K^+K^-J/\psi$ . We also list the  $e^+e^-$  center-of-mass energy ( $\sqrt{s}$ ), number of observed events ( $n^{\text{obs}}$ ), number of backgrounds estimated from  $J/\psi$  mass sidebands ( $n^{\text{bkg}}$ ), detection efficiency ( $\epsilon$ ), and effective ISR luminosity ( $\mathcal{L}$ ). All values are calculated for a 50 MeV bin size and  $\sqrt{s}$  is the central value of the bin. The first errors are statistical and the second ones systematic. For the bins with lower limit at zero at 68.3% confidence interval, a confidence interval is given with systematic error included [26].

$\sqrt{s}$ (GeV)	$n^{\text{obs}}$	$n^{\text{bkg}}$	$\epsilon$ (%)	$\mathcal{L}$ (pb $^{-1}$ )	$\sigma$ (pb)	$\sqrt{s}$ (GeV)	$n^{\text{obs}}$	$n^{\text{bkg}}$	$\epsilon$ (%)	$\mathcal{L}$ (pb $^{-1}$ )	$\sigma$ (pb)
4.175	1	0	1.12	207	$3.6^{+6.2}_{-2.6} \pm 0.3$	5.125	9	2	11.0	286	$2.2^{+1.0}_{-0.8} \pm 0.2$
4.225	1	0	2.25	210	$1.8^{+3.1}_{-1.3} \pm 0.2$	5.175	6	3	11.3	291	$1.3^{+0.8}_{-0.6} \pm 0.1$
4.275	1	2	3.24	214	[0, 2.3]	5.225	5	3	11.6	296	$1.0^{+0.7}_{-0.6} \pm 0.1$
4.325	0	0	4.13	218	[0, 1.3]	5.275	9	7	11.9	301	$1.6^{+0.9}_{-0.8} \pm 0.2$
4.375	0	0	4.91	221	[0, 1.1]	5.325	6	7	12.3	306	$0.8^{+0.8}_{-0.6} \pm 0.1$
4.425	4	0	5.61	225	$2.7^{+1.8}_{-1.2} \pm 0.3$	5.375	17	2	12.6	311	$3.5^{+1.0}_{-1.0} \pm 0.3$
4.475	12	0	6.23	229	$7.1^{+2.6}_{-2.0} \pm 0.6$	5.425	7	7	12.9	317	$1.0^{+0.7}_{-0.6} \pm 0.1$
4.525	8	2	6.78	233	$3.9^{+1.8}_{-1.6} \pm 0.4$	5.475	3	3	13.2	323	$0.4^{+0.5}_{-0.3} \pm 0.1$
4.575	3	2	7.27	237	$1.1^{+1.1}_{-0.8} \pm 0.1$	5.525	7	4	13.5	328	$1.1^{+0.7}_{-0.6} \pm 0.1$
4.625	9	2	7.72	241	$3.8^{+1.8}_{-1.3} \pm 0.3$	5.575	5	4	13.8	334	$0.7^{+0.6}_{-0.4} \pm 0.1$
4.675	7	1	8.13	245	$2.8^{+1.4}_{-1.2} \pm 0.3$	5.625	3	6	14.1	340	[0, 0.7]
4.725	3	3	8.50	249	$0.8^{+1.0}_{-0.6} \pm 0.1$	5.675	4	1	14.4	346	$0.6^{+0.5}_{-0.3} \pm 0.1$
4.775	16	1	8.85	253	$5.9^{+1.7}_{-1.5} \pm 0.5$	5.725	2	3	14.6	353	$0.2^{+0.4}_{-0.2} \pm 0.1$
4.825	2	0	9.18	258	$0.7^{+0.8}_{-0.5} \pm 0.1$	5.775	3	4	14.8	359	$0.3^{+0.5}_{-0.3} \pm 0.1$
4.875	5	2	9.49	262	$1.5^{+1.0}_{-0.8} \pm 0.2$	5.825	4	4	15.0	366	$0.4^{+0.4}_{-0.3} \pm 0.1$
4.925	9	4	9.80	267	$2.5^{+1.2}_{-1.1} \pm 0.2$	5.875	5	6	15.1	373	$0.5^{+0.5}_{-0.4} \pm 0.1$
4.975	12	3	10.1	271	$3.4^{+1.3}_{-1.1} \pm 0.3$	5.925	4	5	15.2	380	$0.3^{+0.5}_{-0.3} \pm 0.1$
5.025	7	4	10.4	276	$1.7^{+1.0}_{-0.9} \pm 0.2$	5.975	3	4	15.3	387	$0.2^{+0.4}_{-0.2} \pm 0.1$
5.075	11	2	10.7	281	$2.9^{+1.1}_{-1.0} \pm 0.3$						

TABLE II. Cross sections ( $\sigma$ ) of  $e^+e^- \rightarrow K_S^0 K_S^0 J/\psi$ . We also list the  $e^+e^-$  center-of-mass energy ( $\sqrt{s}$ ), number of observed events ( $n^{\text{obs}}$ ), number of backgrounds estimated from  $J/\psi$  mass sidebands ( $n^{\text{bkg}}$ ), detection efficiency ( $\epsilon$ ), and effective ISR luminosity ( $\mathcal{L}$ ). All values are calculated for a 50 MeV bin size and  $\sqrt{s}$  is the central value of the bin. As the number of  $K_S^0 K_S^0 J/\psi$  signal events is small, a 68.3% confidence interval for the measured cross section is given with systematic error included [26].

$\sqrt{s}$ (GeV)	$n^{\text{obs}}$	$n^{\text{bkg}}$	$\epsilon$ (%)	$\mathcal{L}$ (pb $^{-1}$ )	$\sigma$ (pb)	$\sqrt{s}$ (GeV)	$n^{\text{obs}}$	$n^{\text{bkg}}$	$\epsilon$ (%)	$\mathcal{L}$ (pb $^{-1}$ )	$\sigma$ (pb)
4.175	0	0	0.26	207	[0, 21]	5.125	0	0	0.96	286	[0, 4.0]
4.225	0	0	0.30	210	[0, 18]	5.175	1	1	1.00	291	[0, 6.7]
4.275	0	0	0.34	214	[0, 16]	5.225	0	0	1.03	296	[0, 3.6]
4.325	0	1	0.37	218	[0, 10]	5.275	1	0	1.07	301	[0.7, 7.1]
4.375	0	0	0.41	221	[0, 13]	5.325	2	2	1.11	306	[0.7, 8.7]
4.425	1	0	0.44	225	[2.5, 23]	5.375	0	1	1.15	311	[0, 2.2]
4.475	0	0	0.48	229	[0, 10]	5.425	0	0	1.18	317	[0, 3.0]
4.525	0	0	0.52	233	[0, 9.2]	5.475	0	1	1.22	323	[0, 2.0]
4.575	0	0	0.55	237	[0, 8.4]	5.525	1	1	1.26	328	[0, 4.7]
4.625	0	0	0.59	241	[0, 7.8]	5.575	1	3	1.30	334	[0, 3.4]
4.675	0	1	0.63	245	[0, 5.0]	5.625	0	5	1.34	340	[0, 1.0]
4.725	2	1	0.66	249	[2.5, 20]	5.675	0	2	1.37	346	[0, 1.3]
4.775	0	0	0.70	253	[0, 6.2]	5.725	1	1	1.41	353	[0, 3.9]
4.825	1	2	0.74	258	[0, 8.5]	5.775	0	2	1.45	359	[0, 1.2]
4.875	1	2	0.77	262	[0, 7.9]	5.825	0	2	1.49	366	[0, 1.1]
4.925	1	0	0.81	267	[1.1, 11]	5.875	0	2	1.53	373	[0, 1.1]
4.975	0	1	0.85	271	[0, 3.3]	5.925	1	4	1.56	380	[0, 2.5]
5.025	1	0	0.89	276	[1.0, 9.4]	5.975	0	3	1.60	387	[0, 0.7]
5.075	0	0	0.92	281	[0, 4.3]						

TABLE III. Systematic errors in  $e^+e^- \rightarrow K^+K^-J/\psi$  and  $K_S^0K_S^0J/\psi$  cross section measurements.

Source	$K^+K^-J/\psi$ (%)	$K_S^0K_S^0J/\psi$ (%)
Particle identification	3.6	2.6
Tracking	3.3	0.7
$K_S^0$ selection	...	5.6
$J/\psi$ mass and $M_{\text{rec}}^2$ selection	0.4	0.4
Background estimation	2.6	14
Integrated luminosity	1.4	1.4
Generator	4.8	4.5
Trigger efficiency	1.0	1.0
Branching fractions	1.0	1.0
MC statistics	1.5	1.5
Sum in quadrature	7.8	16

MC simulations and no evidence is found for non- $S$  wave components. The selected data sample contains at least four charged tracks and so the trigger efficiency is higher than 98% according to MC simulation. A 1.0% systematic error is assigned for the trigger uncertainty. The uncertainty of  $\mathcal{B}(J/\psi \rightarrow \ell^+\ell^-) = \mathcal{B}(J/\psi \rightarrow e^+e^-) + \mathcal{B}(J/\psi \rightarrow \mu^+\mu^-)$  is taken as 1.0% from Ref. [14]. The uncertainty of  $\mathcal{B}(K_S^0 \rightarrow \pi^+\pi^-)$  is neglected. Finally, the MC statistical error on the efficiency is 1.5%. Assuming that all the sources are independent and adding them in quadrature, we obtain a total systematic error on the cross section of 7.8% for the  $K^+K^-J/\psi$  and 16% for  $K_S^0K_S^0J/\psi$  final states.

#### IV. RESONANT STRUCTURES

The unbinned maximum likelihood fit performed in Ref. [13] is applied to the  $K^+K^-J/\psi$  mass spectrum in Fig. 2(a). The theoretical shape is multiplied by the efficiency and effective luminosity, which are functions of the  $K^+K^-J/\psi$  invariant mass. The BW function for a spin-1 resonance decaying into a final state  $f$  with mass  $M$ , total width  $\Gamma_{\text{tot}}$  and partial width  $\Gamma_{e^+e^-}$  to  $e^+e^-$  is

$$\sigma(s) = \frac{M^2 12\pi\Gamma_{e^+e^-}\mathcal{B}(R \rightarrow f)\Gamma_{\text{tot}}\rho(\sqrt{s})}{s (s - M^2)^2 + M^2\Gamma_{\text{tot}}^2} \rho(M),$$

where  $\mathcal{B}(R \rightarrow f)$  is the branching fraction of the resonance to the final state  $f$ , and  $\rho(\sqrt{s})$  is the three-body decay phase space factor for  $X \rightarrow K^+K^-J/\psi$ . We attempt to fit the  $K^+K^-J/\psi$  invariant mass spectrum using two different parametrizations of the signal shape: (1) a single BW function plus a background term; (2) a coherent sum of a BW function and a  $\psi(4415)$  component with mass and width fixed at their world average values [14] plus a background term. The fit results are shown in Fig. 5. The results of the fit for the BW parameters [ $M = (4482 \pm 45)$  MeV/ $c^2$ ,  $\Gamma_{\text{tot}} = (432 \pm 56)$  MeV/ $c^2$  for model (a) and  $M = (4747 \pm 117)$  MeV/ $c^2$ ,  $\Gamma_{\text{tot}} = (671 \pm 86)$  MeV/ $c^2$  for model (b)] are consistent with the previously published results within about  $2\sigma$ , but the goodness of the fit [ $\chi^2/ndf = 39/13 = 3.0$  for model (a) and  $\chi^2/ndf = 30/11 = 2.7$  for model (b)] is marginal. (Here,  $ndf$  is the number of degrees of freedom.) Thus, our two models cannot describe the data well with the increased statistics. Here, in determining the goodness of each fit, we bin the data so that the expected number of events in a bin is at least 7. Adding a coherent  $Y(4260)$  amplitude in the fit with mass and width fixed at the latest Belle measurement [1] yields an upper limit on  $\mathcal{B}(Y(4260) \rightarrow K^+K^-J/\psi)\Gamma(Y(4260) \rightarrow e^+e^-) < 1.7$  eV/ $c^2$  at 90% confidence level. A similar fit to the  $K_S^0K_S^0J/\psi$  invariant mass spectrum with a  $Y(4260)$  amplitude yields an upper limit on  $\mathcal{B}(Y(4260) \rightarrow K_S^0K_S^0J/\psi)\Gamma(Y(4260) \rightarrow e^+e^-) < 0.85$  eV/ $c^2$  at 90% confidence level.

Possible intermediate states are studied by examining the Dalitz plot of the selected  $K^+K^-J/\psi$  candidate events. Figure 6 shows the Dalitz plots of events in the  $J/\psi$  signal region and  $J/\psi$  mass sidebands. Figure 7 shows a projection of the  $M(K^+K^-)$ ,  $M(K^+J/\psi)$ , and  $M(K^-J/\psi)$  invariant mass distributions. Background events estimated from the normalized  $J/\psi$  mass sidebands are shown as the

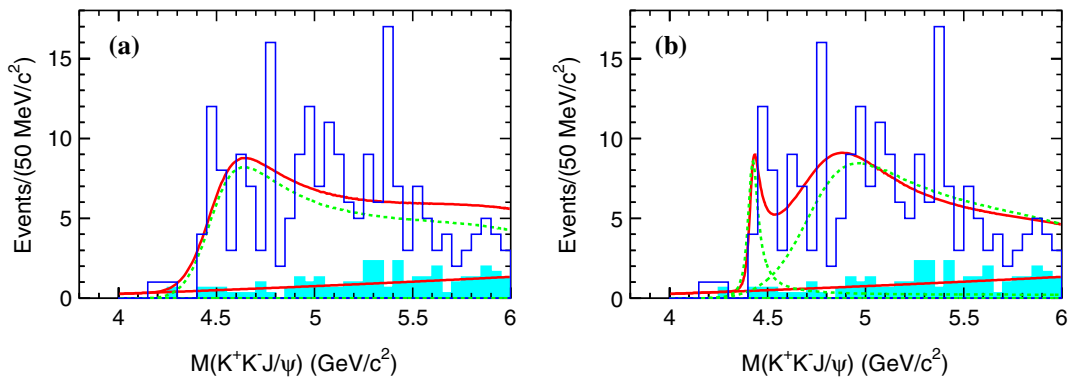


FIG. 5 (color online). Fits to the  $K^+K^-J/\psi$  invariant mass distribution. The open histograms are the selected data in the  $J/\psi$  signal region while the shaded histograms show the normalized  $J/\psi$  sideband events. The solid curves show the best fit to the data and sideband background with one BW function (a) and the coherent sum of a BW function and the  $\psi(4415)$  component (b).

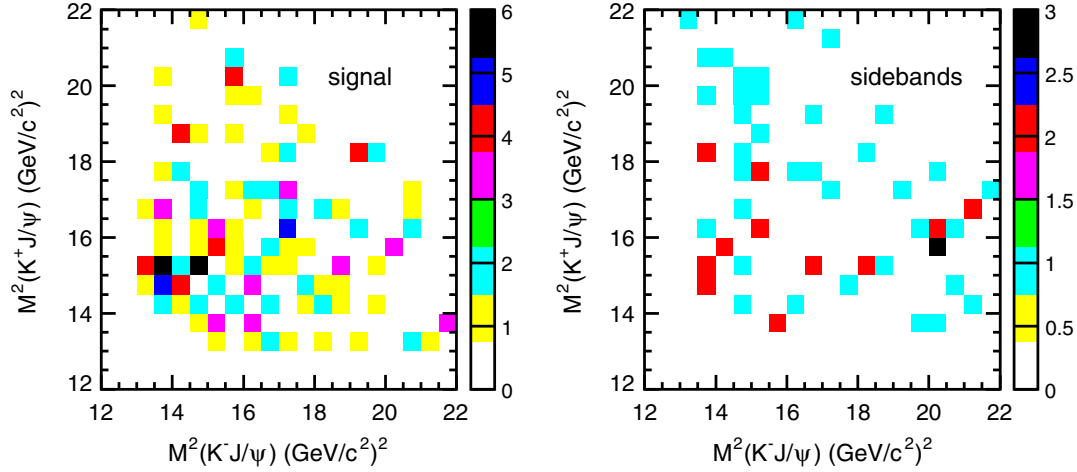


FIG. 6 (color online). Dalitz plots for the selected  $K^+K^-J/\psi$  events for  $4.4 < M(K^+K^-J/\psi) < 5.5 \text{ GeV}/c^2$ . The left panel is for events in the  $J/\psi$  signal region while the right is from the  $J/\psi$  mass sidebands (not normalized).

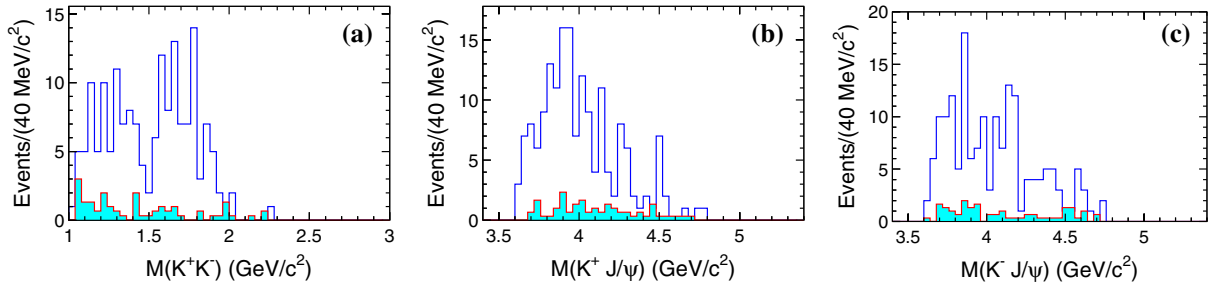


FIG. 7 (color online). Invariant mass distributions of (a)  $K^+K^-$ , (b)  $K^+J/\psi$ , and (c)  $K^-J/\psi$  for  $K^+K^-J/\psi$  events with  $4.4 < M(K^+K^-J/\psi) < 5.5 \text{ GeV}/c^2$ . Solid histograms are for events in the  $J/\psi$  signal region, and the shaded histograms are normalized background from the  $J/\psi$  mass sidebands.

shaded histograms. No obvious structures are observed in the  $K^\pm J/\psi$  system. The low statistics prevent us from extracting additional information on the three-body dynamics.

## V. SUMMARY

The cross sections of  $e^+e^- \rightarrow K^+K^-J/\psi$  and  $K_S^0 K_S^0 J/\psi$  are measured from threshold to 6.0 GeV using the full Belle data sample. There are clear  $K^+K^-J/\psi$  signal events; however fits that were tried before [13] with a smaller data set using either a single BW function or using the  $\psi(4415)$  plus a second BW function are inadequate for the full data sample. Possible intermediate states for the selected  $K^+K^-J/\psi$  events are also investigated by examining the Dalitz plot but no clear structure is observed in the  $K^\pm J/\psi$  system. Since there are only a few  $K_S^0 K_S^0 J/\psi$  signal events and no structure is observed in the  $K_S^0 K_S^0 J/\psi$  mass spectrum, the Dalitz plot of  $K_S^0 K_S^0 J/\psi$  events is not examined. A larger data sample

is necessary to obtain more information about possible structures in the  $K^+K^-J/\psi$ ,  $K_S^0 K_S^0 J/\psi$ ,  $K^+K^-$  and  $K^\pm J/\psi$  systems.

## ACKNOWLEDGMENTS

We thank the KEKB group for excellent operation of the accelerator; the KEK cryogenics group for efficient solenoid operations; and the KEK computer group, the NII, and PNNL/EMSL for valuable computing and SINET4 network support. We acknowledge support from MEXT, JSPS and Nagoya's TLPRC (Japan); ARC and DIISR (Australia); FWF (Austria); NSFC (China); MSMT (Czech Republic); CZF, DFG, and VS (Germany); DST (India); INFN (Italy); MOE, MSIP, NRF, GSDC of KISTI, BK21Plus, and WCU (Korea); MNiSW and NCN (Poland); MES and RFAAE (Russia); ARRS (Slovenia); IKERBASQUE and UPV/EHU (Spain); SNSF (Switzerland); NSC and MOE (Taiwan); and DOE and NSF (USA).



- [1] Z. Q. Liu *et al.* (Belle Collaboration), *Phys. Rev. Lett.* **110**, 252002 (2013).
- [2] M. Ablikim *et al.* (BESIII Collaboration), *Phys. Rev. Lett.* **110**, 252001 (2013).
- [3] T. Xiao, S. Dobbs, A. Tomaradze, and K. K. Seth, *Phys. Lett. B* **727**, 366 (2013).
- [4] F.-K. Guo, C. Hidalgo-Duque, J. Nieves, and M. P. Valderrama, *Phys. Rev. D* **88**, 054007 (2013); L. Maiani, V. Riquer, R. Faccini, F. Piccinini, A. Pilloni, and A. D. Polosa, *Phys. Rev. D* **87**, 111102 (2013); M. Karliner and S. Nussinov, *J. High Energy Phys.* **07** (2013) 153; K. Terasaki, arXiv:1304.7080; E. Braaten, *Phys. Rev. Lett.* **111**, 162003 (2013); C.-F. Qiao and L. Tang, arXiv:1307.6654; Z.-G. Wang and T. Huang, *Phys. Rev. D* **89**, 054019 (2014).
- [5] C.-Y. Cui, Y.-L. Liu, W.-B. Chen, and M.-Q. Huang, *Eur. Phys. J. C* **73**, 2661 (2013); E. Wilbring, H.-W. Hammer, and U.-G. Meißner, *Phys. Lett. B* **726**, 326 (2013); J. R. Zhang, *Phys. Rev. D* **87**, 116004 (2013); Y. Dong, A. Faessler, T. Gutsche, and V. E. Lyubovitskij, *Phys. Rev. D* **88**, 014030 (2013); H.-W. Ke, Z.-T. Wei, and X.-Q. Li, *Eur. Phys. J. C* **73**, 2561 (2013).
- [6] N. Mahajan, arXiv:1304.1301; M. B. Voloshin, *Phys. Rev. D* **87**, 091501 (2013).
- [7] D.-Y. Chen, X. Liu, and T. Matsuki, *Phys. Rev. D* **88**, 036008 (2013); J. M. Dias, F. S. Navarra, M. Nielsen, and C. M. Zanetti, *Phys. Rev. D* **88**, 016004 (2013); X.-H. Liu and G. Li, *Phys. Rev. D* **88**, 014013 (2013); D.-Y. Chen, X. Liu, and T. Matsuki, *Phys. Rev. D* **88**, 014034 (2013); Q.-Y. Lin, X. Liu, and H.-S. Xu, *Phys. Rev. D* **88**, 114009 (2013); D.-Y. Chen, X. Liu, and T. Matsuki, arXiv:1309.4528.
- [8] M. Ablikim *et al.* (BESIII Collaboration), *Phys. Rev. Lett.* **111**, 242001 (2013).
- [9] A. Bondar *et al.* (Belle Collaboration), *Phys. Rev. Lett.* **108**, 122001 (2012).
- [10] S. H. Lee, M. Nielsen, and U. Wiedner, *J. Korean Phys. Soc.* **55**, 424 (2009).
- [11] J. M. Dias, X. Liu, and M. Nielsen, *Phys. Rev. D* **88**, 096014 (2013).
- [12] D.-Y. Chen, X. Liu, and T. Matsuki, *Phys. Rev. Lett.* **110**, 232001 (2013).
- [13] C. Z. Yuan *et al.* (Belle Collaboration), *Phys. Rev. D* **77**, 011105(R) (2008).
- [14] J. Beringer *et al.* (Particle Data Group), *Phys. Rev. D* **86**, 010001 (2012) and 2013 partial update for the 2014 edition.
- [15] S. Kurokawa and E. Kikutani, *Nucl. Instrum. Methods Phys. Res., Sect. A* **499**, 1 (2003), and other papers included in this volume; T. Abe *et al.*, *Prog. Theor. Exp. Phys.* (2013) 03A001 and following articles up to 03A011.
- [16] A. Abashian *et al.* (Belle Collaboration), *Nucl. Instrum. Methods Phys. Res., Sect. A* **479**, 117 (2002); also, see detector section in J. Brodzicka *et al.*, *Prog. Theor. Exp. Phys.* (2012) 04D001.
- [17] G. Rodrigo, H. Czyż, J. H. Kühn, and M. Szopa, *Eur. Phys. J. C* **24**, 71 (2002).
- [18] J. Z. Bai *et al.* (BES Collaboration), *Phys. Rev. D* **62**, 032002 (2000).
- [19] E. Nakano, *Nucl. Instrum. Methods Phys. Res., Sect. A* **494**, 402 (2002).
- [20] K. Hanagaki, H. Kakuno, H. Ikeda, T. Iijima, and T. Tsukamoto, *Nucl. Instrum. Methods Phys. Res., Sect. A* **485**, 490 (2002).
- [21] A. Abashian *et al.*, *Nucl. Instrum. Methods Phys. Res., Sect. A* **491**, 69 (2002).
- [22] F. Fang, Ph. D. thesis, University of Hawaii, 2003, <http://belle.kek.jp/bdocs/theses.html>.
- [23] In this paper,  $M(K^+K^-\ell^+\ell^-) - M(\ell^+\ell^-) + m_{J/\psi}$  is used instead of the invariant mass of the four final state particles to improve the mass resolution. Here,  $m_{J/\psi}$  is the nominal mass of the  $J/\psi$  meson. The same is true for the  $M(K_S^0K_S^0\ell^+\ell^-)$  calculation.
- [24] K. Zhu, C. Z. Yuan, and R. G. Ping, *Phys. Rev. D* **78**, 036004 (2008).
- [25] E. A. Kuraev and V. S. Fadin, *Yad. Fiz.* **41**, 733 (1985); [*Sov. J. Nucl. Phys.* **41**, 466 (1985)].
- [26] J. Conrad, O. Botner, A. Hallgren, and C. Perez de los Heros, *Phys. Rev. D* **67**, 012002 (2003).